Inorg. Chem. **2007**, *46*, 3083–3088

Thermal and Electrochemically Assisted Pd–Cl Bond Cleavage in the d^9–d^9 $Pd_2(dppm)_2Cl_2$ Complex by $Pd_3(dppm)_3(CO)^{n+}$ Clusters ($n = 2, 1, 0$)

Cyril Cugnet,[1a] Yves Mugnier,*[,1a] Sophie Dal Molin,[1a] David Brevet,[1a] Dominique Lucas,[1a] and Pierre D. Harvey*[,1b]

Institut de Chimie Moléculaire de l'Université de Bourgogne, (ICMUB) UMR CNRS 5260, Université de Bourgogne, Faculté des Sciences Mirande, 9 Allée A. Savary, 21000 Dijon, France, and Département de Chimie, Université de Sherbrooke, Sherbrooke, Québec, Canada J1K 2R1

Received September 19, 2006

A new aspect of reactivity of the cluster $[Pd_3(dppm)_3(\mu^3\text{-CO})]^{n+}$, ($[Pd_3]^{n+}$, $n = 2, 1, 0$) with the low-valent metal–metal-bonded $Pd_2(dppm)_2Cl_2$ dimer (Pd_2Cl_2) was observed using electrochemical techniques. The direct reaction between $[Pd_3]^{2+}$ and Pd_2Cl_2 in THF at room temperature leads to the known $[Pd_3(dppm)_3(\mu^3\text{-CO})(Cl)]^+$ ($[Pd_3(Cl)]^+$) adduct and the monocationic species $Pd_2(dppm)_2Cl^+$ (very likely as $Pd_2(dppm)_2(Cl)(THF)^+$, $[Pd_2Cl]^+$) as unambiguously demonstrated by UV–vis and ^{31}P NMR spectroscopy. In this case, $[Pd_3]^{2+}$ acts as a strong Lewis acid toward the labile Cl^- ion, which weakly dissociates from Pd_2Cl_2 (i.e., dissociative mechanism). Host–guest interactions between $[Pd_3]^{2+}$ and Pd_2Cl_2 seem unlikely on the basis of computer modeling because of the strong screening of the Pd–Cl fragment by the Ph-dppm groups in Pd_2Cl_2. The electrogenerated clusters $[Pd_3]^+$ and $[Pd_3]^0$ also react with Pd_2Cl_2 to unexpectedly form the same oxidized adduct, $[Pd_3(Cl)]^+$, despite the known very low affinity of $[Pd_3]^+$ and $[Pd_3]^0$ toward Cl^- ions. The reduced biproduct in this case is the highly reactive zerovalent species "$Pd_2(dppm)_2$" or "Pd(dppm)" as demonstrated by quenching with $CDCl_3$ (forming the well-known complex $Pd(dppm)Cl_2$) or in presence of dppm (forming the known $Pd_2(dppm)_3$ d^{10}–d^{10} dimer). To bring these halide-electron exchange reactions to completion for $[Pd_3]^+$ and $[Pd_3]^0$, 0.5 and 1.0 equiv of Pd_2Cl_2 are necessary, respectively, accounting perfectly for the number of exchanged electrons. The presence of a partial dissociation of Pd_2Cl_2 into the Cl^- ion and the monocation $[Pd_2Cl]^+$, which is easier to reduce than Pd_2Cl_2, is suggested to explain the overall electrochemical results. It is possible to regulate the nature of the species formed from Pd_2Cl_2 by changing the state of charge of the title cluster.

Introduction

Homogeneous catalytic processes using transition metal complexes often require a key step of activation of the so-called precatalyst. This primary step may be an abstraction of a blocking halide ligand or an electron-transfer generating what is often referred to as the active catalyst. Recently, our groups reported an exhaustive series of reactivity and properties of the title clusters (Chart 1),[2] including host–guest behavior,[2d] electrocatalytically induced C–X bond activation (X = Cl, Br, I), and electrocatalysis (for the formation of acid fluorides, dissymmetric esters and ethers, diradical couplings, and C–H bond activation).[3] While these investigations focused on organic substrates, the inorganic counterpart (M–X) was neglected. The abstraction of a Cl^- ligand of M–X (X = Cl) by the $[Pd_3(dppm)_3(\mu^3\text{-CO})]^{2+}$ cluster to form the known adduct $[Pd_3(dppm)_3(\mu^3\text{-CO})(Cl)]^+$ ($[Pd_3(Cl)]^+$) yielding the monocation derivative M^+ represents an interesting avenue for catalysis because the Cl^- ions

* To whom correspondence should be addressed. Phone/Fax: 33 (0)3 80 39 60 91 (Y.M.). E-mail: yves.mugnier@u-bourgogne.fr (Y.M.); pierre.harvey@usherbrooke.ca (P.D.H.). Phone: (819) 821-7092 (P.D.H.). Fax: (819) 821-8017 (P.D.H.).
(1) (a) Université de Bourgogne. (b) Université de Sherbrooke.

(2) (a) Cugnet, C.; Lucas, D.; Lemaître, F.; Collange, E.; Soldera, A.; Mugnier, Y.; Harvey, P. D. *Chem.—Eur. J* **2006**, *12*, 8386–8395. (b) Brevet, D.; Lucas, D.; Richard, P.; Vallat, A.; Mugnier, Y.; Harvey, P. D. *Can. J. Chem.* **2006**, *84*, 243. (c) Brevet, D.; Lucas, D.; Mugnier, Y.; Harvey, P. D. *J. Cluster Sci.* **2006**, *17*, 5. (d) Harvey, P. D.; Mugnier, Y.; Lucas, D.; Evrard, D.; Lemaître, F.; Vallat, A. *J. Cluster Sci.* **2004**, *15*, 63 and references therein. (e) Lemaitre, F.; Lucas, D.; Brevet, D.; Vallat, A.; Harvey, P. D.; Mugnier, Y. *Inorg. Chem.* **2002**, *41*, 2368.

10.1021/ic061777h CCC: $37.00
Published on Web 03/20/2007

Chart 1

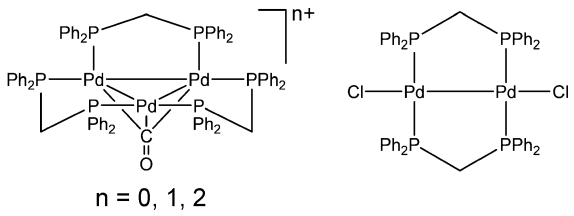

can be subsequently removed in a catalytic fashion.[3b] So, this cluster can act as a cocatalyst.

We now wish to report the reactivity of $[Pd_3(dppm)_3(\mu^3\text{-}CO)]^{n+}$, ($[Pd_3]^{n+}$, $n = 2, 1, 0$) toward $Pd_2(dppm)_2Cl_2$ (Pd_2Cl_2)(Chart 1).

Experimental Section

Materials. $[Pd_3(dppm)_3(\mu^3\text{-}CO)](PF_6)_2$,[4] $Pd_2(dppm)_2Cl_2$,[5] and $Pd(dppm)Cl_2$[6] were prepared according to literature procedures. All solvents were dried under argon, and all experiments were performed under argon.

Electrochemical Experiments. All manipulations were performed using Schlenk techniques in an atmosphere of dry oxygen-free argon gas. The supporting electrolyte was degassed under vacuum before use and then solubilized at a concentration of 0.2 mol L^{-1}. For cyclic voltammetry experiments, the concentration of the analyte was approximatively 10^{-3} mol L^{-1}. Voltammetric analyses were carried out in a standard three-electrode cell with an EG & G Princeton Applied Research (PAR) Model 263A potentiostat connected to an interfaced computer employing Electrochemistry Power Suite software. The reference electrode was a saturated calomel electrode (SCE) separated from the solution by a sintered glass disk. The auxiliary electrode was a platinum wire. For all voltammetric measurements, the working electrode was a vitreous carbon electrode ($\Phi = 3$ mm), and the angular velocity was 26.5 rad s^{-1}. In these conditions, when operated in THF, the formal potential for the ferrocene $\pm$ couple is found to be +0.56 V versus SCE. The controlled potential electrolysis was performed with an Amel 552 potentiostat coupled with an Amel 721 electronic integrator. High-scale electrolyses were performed in a cell with three compartments separated with fritted glasses of medium porosity. Carbon gauze was used as the working electrode; a platinum plate was emplyed as the counter-electrode, and a saturated calomel electrode was used as the reference electrode.

Spectroscopy. The ^{31}P NMR spectra were recorded on a 600 MHz BRUKER Avance II NMR spectrometer. The chemical shifts are reported with respect to H_3PO_4. Mass spectra were obtained on a Bruker Daltonics Ultraflex II spectrometer (MALDI-TOF) using dithranol as a matrix.

$[Pd_2(dppm)_2(Cl)(THF)]^+$. One equivalent of $AgPF_6$ (2.4 mg, 9.5 μmol) was added to a solution of $Pd_2(dppm)_2Cl_2$ (10 mg, 9.5 μmol) in THF (5 mL). The orange solution turned dark orange immediately, and an AgCl precipitate was formed. RMN $^{31}P\{^1H\}$ (600 MHz, acetone-d_6, 20 °C): δ 2.05 (t), −5.3 (t, $J = 43.5$ Hz). (+) MALDI-TOF MS: *m*/*z* (assignment, relative intensity) 982 ($Pd_2(dppm)_2$, 100%), 995 ($Pd_2(dppm)_2O$, 18.5%), 1017 ($Pd_2(dppm)_2$-Cl, 6.5%), 1052 ($Pd_2(dppm)_2Cl_2$ residue).

$[Pd_2(dppm)_2(Cl)(MeCN)]^+$. One equivalent of $AgPF_6$ (2.4 mg, 9.5μmol) was added to a solution of Pd2$(dppm)_2Cl_2$ (10 mg, 9.5.μmol) in MeCN (5 mL). The orange solution turned yellow immediately, and an AgCl precipitate was formed. RMN $^{31}P\{^1H\}$ (600 MHz, acetone-d_6, 20 °C): δ 1.6 (t), −5.5 (t, $J = 42.5$ Hz). (+) MALDI-TOF MS: *m*/*z* (assignment, relative intensity) 982 ($Pd_2(dppm)_2$, 100%), 995 ($Pd_2(dppm)_2O$, 8.3%), 1017 ($Pd_2(dppm)_2$-Cl, 6.7%), 1052 ($Pd_2(dppm)_2Cl_2$ residue).

Modeling. The computer modeling was performed using the commercial software PC-Model from Serena Software. It uses a MMX force field for all atoms.

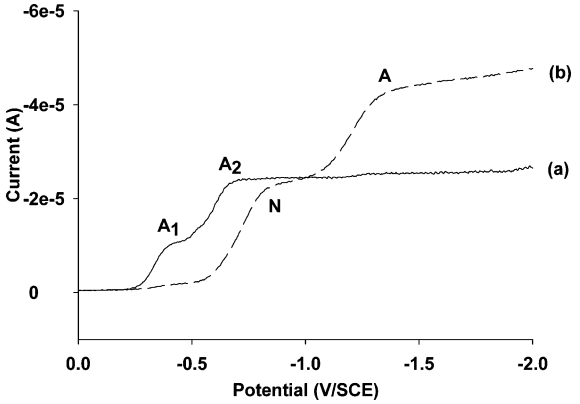

Figure 1. (a) RDE voltammograms of $[Pd_3]^{2+}$ (scan rate = 0.02 V s^{-1}) in a THF/Bu_4NPF_6 solution at room temperature and (b) after the addition of 1 equiv of Pd_2Cl_2. Starting potential: 0 V.

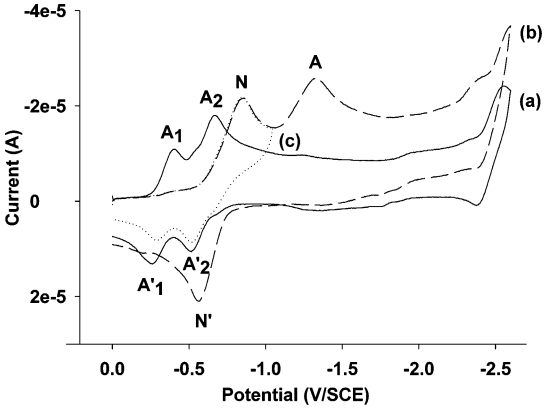

Figure 2. (a) Cyclic voltammograms of $[Pd_3]^{2+}$ (scan rate = 0.1 V s^{-1}) in a THF/Bu_4NPF_6 solution at room temperature and (b and c) after the addition of 1 equiv of Pd_2Cl_2. Starting potential: 0 V. Inversion potential: (a and b) −2.5, (c) −1 V.

Results and Discussion

The voltammetric measurements, made using a rotating disk electrode (RDE) for the $[Pd_3]^{2+}$ cluster in THF and in the presence of 0.2 mol L^{-1} Bu_4NPF_6 as the supporting electrolyte, exhibit two reduction waves A_1 and A_2 at −0.29 and −0.51 V versus SCE (Figure 1, trace a). The cyclic voltammogram (CV) (Figure 2, trace a) exhibits the same electrochemical processes as reversible systems (A_1/A'_1 and

(3) (a) Lucas, D.; Lemaître, F.; Gallego-Gomez, B.; Cugnet, C.; Richard, P.; Mugnier, Y.; Harvey, P. D. *Eur. J. Inorg. Chem.* **2005**, 1011. (b) Lemaître, F.; Lucas, D.; Groison, K.; Richard, P.; Mugnier, Y.; Harvey, P. D. *J. Am. Chem. Soc.* **2003**, *125*, 5511. (c) Brevet, D.; Mugnier, Y.; Lemaître, F.; Lucas, D.; Samreth, S.; Harvey, P. D. *Inorg. Chem.* **2003**, *42*, 4910. (d) Lemaître, F.; Lucas, D.; Mugnier, Y.; Harvey, P. D. *J. Org. Chem.* **2002**, *67*, 7537. (e) Brevet, D.; Lucas, D.; Cattey, H.; Lemaitre, F.; Mugnier, Y.; Harvey, P. D. *J. Am. Chem. Soc.* **2001**, *123*, 4340.
(4) Manojlovic-Muir, L.; Muir, K. W.; Lloyd, B. R.; Puddephatt, R. J. *J. Chem. Soc., Chem. Commun.* **1983**, 1336.
(5) Benner, L. S.; Balch, A. L. *J. Am. Chem. Soc.* **1978**, *100*, 6099.

Chart 2

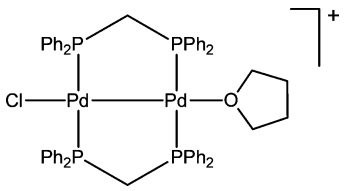

A_2/A'_2), which allows for the description of the following redox reactions[6]

$$[Pd_3]^{2+} + e^- \overset{(A_1/A'_1)}{\rightleftharpoons} [Pd_3]^+ \quad (1)$$

$$[Pd_3]^+ + e^- \overset{(A_2/A'_2)}{\rightleftharpoons} [Pd_3]^0 \quad (2)$$

In this way, cluster species $[Pd_3]^+$ and $[Pd_3]^0$ can be electrochemically generated in the electrochemical cell prior to the addition of Pd_2Cl_2.

Reactivity of $[Pd_3]^{2+}$ toward Pd_2Cl_2. In the presence of one equivalent of Pd_2Cl_2, drastic modifications of the $[Pd_3]^{2+}$ RDE voltammogram are readily observed. The reduction waves A_1 and A_2 disappear, and two well-defined reduction waves N and A are observed. Wave A corresponds to the reduction of Pd_2Cl_2.[7] The current amplitude of wave N is equal to the sum of heights of wave A_1 and A_2 (Figure 1). A well defined absorption band is observed at 460 nm in UV−vis spectra which corresponds to the adduct $[Pd_3(Cl)]^+$.[3b,d,e] In addition, after evaporation of the THF solvent, the ^{31}P NMR spectrum of the crude product exhibits several signals, one of which is a sharp singlet at −9.8 ppm which confirms the presence of $[Pd_3(Cl)]^+$; this value was also obtained by addition of Cl^- anion (Bu_4NCl) to a solution containing the title cluster.[8] An independent NMR-tube reaction of $[Pd_3]^{2+}$ with Pd_2Cl_2 monitored by ^{31}P NMR gives the same result as above.

The presence of wave A in the resulting solution appears odd at first glance because waves A_1 and A_2 disappear (i.e., $[Pd_3]^{2+}$ is totally consumed), indicating that a fast reactivity between $[Pd_3]^{2+}$ and Pd_2Cl_2 occurs, whereas the reduction wave A (reduction of Pd_2Cl_2) is still present, and no new wave is observed attributable to the biproduct of $[Pd_3(Cl)]^+$. In the CV, the oxidation peaks A'_1 and A'_2 are observed (i.e., $[Pd_3]^0$ is present) when the scan is reversed after peak N (Figure 2, trace b) but are absent when the scan is reversed after −2.6 V (i.e., $[Pd_3]^0$ is absent) and a well-defined oxidation peak N′ is depicted.

The presence of $[Pd_3(Cl)]^+$ indicates an heterolytic Pd−Cl bond cleavage in Pd_2Cl_2 yielding $[Pd_2Cl]^+$ (Chart 2) in which the THF ligand is most likely coordinated to the palladium atom according to the following reaction

$$[Pd_3]^{2+} + Pd_2(dppm)_2Cl_2 \xrightarrow[THF]{} [Pd_3(Cl)]^+ + Pd_2(dppm)_2Cl(THF)^+ \quad (3)$$

Coordination of a neutral ligand at the axial position of the $Pd_2(dppm)_2^{2+}$ fragment is not uncommon. For example, the disubstituted complex $Pd_2(dppm)_2(NCCH_3)_2^{2+}$ is known,[9] along with the dissymmetric dimer $Pd_2(dppm)_2(Cl)(NC_5H_4\text{-}2\text{-}CHCH_2)^+$.[10]

The ^{31}P NMR spectra of the crude product also exhibit two pseudo-triplets centered at 2.05 and −5.3 ppm; this is best described as a AA′BB′ system that approximates a A_2B_2 spin system where the coupling constants are very similar (J = 43.5 Hz) as for the known dissymmetric dimers $Pd_2(dppm)_2(Cl)(I)$ and $Pd_2(dppm)_2(Br)(I)$ (J = 39 Hz).[11] In a case where the J values are different, the spin system is best described as AA′BB′ similar to that observed for dissymmetric dimer $Pd_2(dppm)_2(Br)(Cl)$ (J = 39 Hz).[11] From this observed reactivity, one can readily conclude that $[Pd_3]^{2+}$ is a stronger Lewis acid for Cl^- than the unsaturated intermediate $[Pd_2(Cl)]^+$.

The unexpected presence of wave A in trace b (Figure 2) is caused by $[Pd_3(Cl)]^+$ being reduced to $[Pd_3]^0$ by a 2-electron process, which has no affinity for the Cl^- ion.[3b,e] So, these anions are released according to

$$[Pd_3(Cl)]^+ + 2e^- \rightarrow [Pd_3]^0 + Cl^- \quad (4)$$

Then these released Cl^- ions are captured by $[Pd_2Cl]^+$ according to eq 5, and Pd_2Cl_2 is regenerated

$$Pd_2(dppm)_2Cl(THF)^+ + Cl^- \rightarrow Pd_2(dppm)_2Cl_2 + THF \quad (5)$$

Therefore, after scanning is completed through peak N, derivatives $[Pd_3]^0$ and Pd_2Cl_2 are formed, and $[Pd_3]^0$ can be oxidized back to $[Pd_3]^{2+}$ according to eqs 1 and 2 (oxidation peaks A'_1 and A'_2, see Figure 2) during the anodic scan. When the anodic sweep is started at −2.6 V, only oxidation peak N′ is observed. This peak corresponds to the oxidation of $[Pd_3]^0$ under the influence of Cl^- (process ECE, electrochemical/chemical/electrochemical)[2d] which is formed by reduction of Pd_2Cl_2 at the potential of peak A.

We also considered a host−guest interaction, but this hypothesis should readily be discarded because the Cl atom in Pd_2Cl_2 is far too encumbered by the dppm-phenyl groups where obviously strong steric interactions with $[Pd_3]^{2+}$ occur. This feature is unambiguously demonstrated by computer modeling (Figure 3). Instead, a dissociative mechanism must be taken into account, as shown in eq 6

$$Pd_2(dppm)_2Cl_2 + THF \rightleftharpoons Pd_2(dppm)_2Cl(THF)^+ + Cl^- \quad (6)$$

This proposal is entirely consistent with the relatively facile ligand substitution reaction known for Pd_2Cl_2 and related

(6) Gauthron, I.; Mugnier, Y.; Hierso, K.; Harvey, P. D. *Can. J. Chem.* **1997**, *75*, 1182.
(7) Gauthron, I.; Mugnier, Y.; Hierso, K.; Harvey, P. D. *New J. Chem.* **1998**, 247.
(8) Lloyd, B. R.; Manojlovic-Muir, L.; Muir, K. W.; Puddephatt, R. J. *Organometallics* **1993**, *12*, 1231−1237.
(9) (a) Miedaner, A.; DuBois, D. L. *Inorg. Chem.* **1988**, *27*, 2479. (b) Murahashi, T.; Nagai, T.; Okuno, T.; Matsutani, T.; Kurosawa, H. *Chem. Comm.* **2000**, 1689.
(10) Maekawa, M.; Munakata, M.; Kuroda-Sowa, T.; Suenaga, Y. *Polyhedron* **1998**, *17*, 3657.
(11) Hunt, C. T.; Balch, A. L. *Inorg. Chem.* **1982**, *21*, 1641.

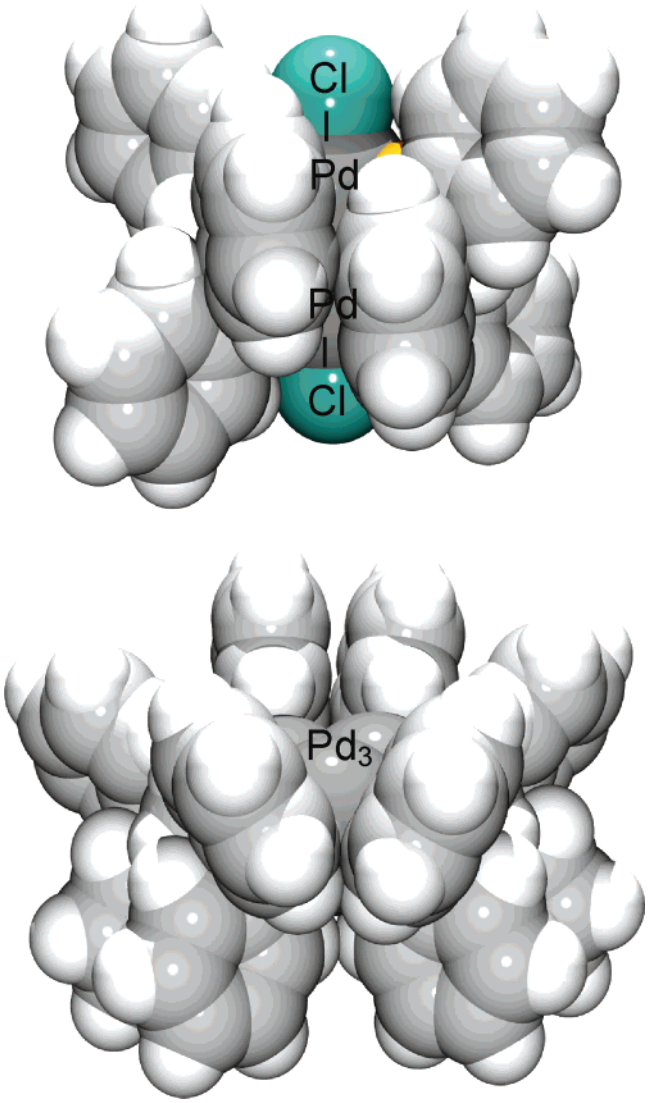

Figure 3. Space filling models for $\mathbf{1}^{2+}$ and **2** showing the screening of the Cl ligand on **2** preventing good interactions with the Pd_3 center. This conformation is the one that shows the largest possible cavity size. This global conformation depends on the dppm conformation.

complexes.[5,12] Subsequently, the free Cl^- ion is scavenged by $[Pd_3]^{2+}$

$$[Pd_3]^{2+} + Cl^- \rightarrow [Pd_3(Cl)]^+ \qquad (7)$$

To check this hypothesis, the reactivity of Pd_2Cl_2 in the presence of $AgPF_6$ in THF was also investigated. The ^{31}P NMR spectrum exhibits the same pseudo-triplets described above, in agreement with the formation of $[Pd_2Cl]^+$.[13] When the reaction occurs in MeCN, two different pseudo-triplets are also observed at 1.6 and −5.5 ppm. These values differ from that observed for eq 4 described above **(**$J = 42.5$ Hz**)**. Moreover this cationic species, prepared in THF or MeCN, was characterized by MALDI-TOF mass spectrometry. We

(12) For example, see: Kullberg, M. L.; Lemke, F. R.; Powell, D. R.; Kubiak, C. P. *Inorg. Chem.* **1985**, *24*, 3589.
(13) When Ag^+ ($AgPF_6$) is added to the solution containing Pd_2Cl_2, a reduction wave at −0.55 V appears, which corresponds to the reduction of $[Pd_2Cl]^+$.

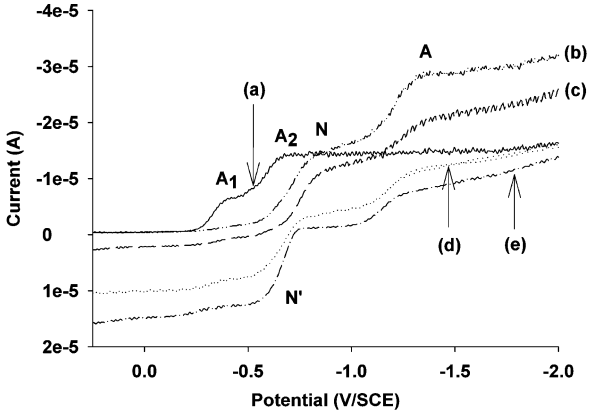

Figure 4. (a) RDE voltammograms of $[Pd_3]^{2+}$ (scan rate = 0.02 V s^{-1}) in THF/Bu_4NPF_6 solution at room temperature and after (b) the addition of 1 equiv of Pd_2Cl_2, (c) 1-electron reduction at −0.8 V, (d) 2-electron reduction at −0.8 V, and (e) 2.6-electron reduction at −0.8 V. Starting potential: 0.2 V

can observe two signals at 982 (100%) and 1017 (6.5%) associated to fragments $Pd_2(dppm)_2^+$ and $Pd_2(dppm)_2Cl^+$.

Coulometric measurements at peak N (for the adduct $[Pd_3(Cl)]^+$) do not provide the expected transfer of 2 electrons as suggested by eq 4, but rather, values varying between 2.6 and 3 were obtained. An example of evolution of RDE voltammograms is shown in Figure 4.

After a one-electron reduction, no oxidation wave in the range potential of wave N is observed. However after consumption of two electrons, a well-defined oxidation wave N′ appears. Its current intensity increases as the quantity of electricity consumed increases, even for a quantity of electricity exceeding two electrons (see entries for 2.6 electrons). Moreover, the reduction wave A is still present, but its current intensity is smaller than the initial wave prior to electrolysis. One question that comes to mind is why are the peaks A'_1 and A'_2 obtained in the CV (Figure 2, trace c) but do not appear after the electrolysis (Figure 3). To answer this question, the reactivity of Pd_2Cl_2 toward the electrogenerated paramagnetic $[Pd_3]^+$ and zerovalent species $[Pd_3]^0$ was investigated because no real affinity exists between these low-valent species and Cl^- anions.

Reactivity of $[Pd_3]^+$ toward Pd_2Cl_2. Figure 5 shows the RDE voltammograms of the electrogenerated $[Pd_3]^+$ which exhibits an oxidation wave, A'_1 (reverse reaction of eq 1) and a reduction wave, A_2 (Figure 5, trace b). When one equivalent of Pd_2Cl_2 is added, drastic modifications are readily observed. Waves A'_1 and A_2 disappear and reduction waves N_1 and A appear (Figure 5, trace c). After a two electron reduction at −0.9 V (plateau of wave N_1), the oxidation wave N_1', which is well defined, and reduction wave A are observed (Figure 5, trace d). The reaction is complete in $[Pd_3]^+$, but dimer Pd_2Cl_2 is still present (wave A).

When 0.5 equiv of Pd_2Cl_2 is used (instead of 1 equiv), the reaction also reaches completion (disappearance of $[Pd_3]^+$), and wave A disappears as well. In both cases, no EPR signal is detected, confirming not only that $[Pd_3]^+$, a paramagnetic cluster, is totally consumed but also that no other paramagnetic species is formed. In addition, both

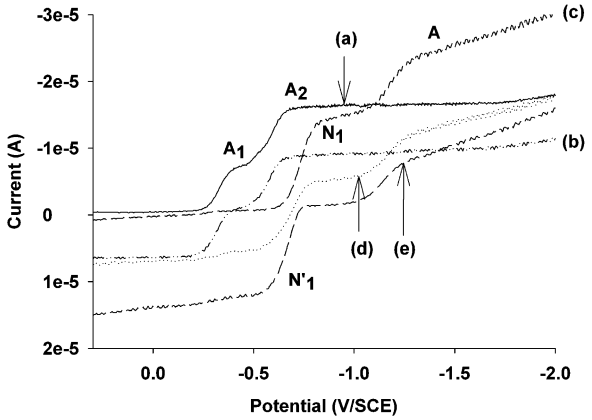

Figure 5. (a) RDE voltammograms of $[Pd_3]^{2+}$ (scan rate = 0.02 V s^{-1}) in THF/Bu_4NPF_6 solution at room temperature, (b) after 1-electron reduction at −1 V producing $[Pd_3]^+$, and of the (c) solution from trace b after the addition of 1 equiv of Pd_2Cl_2, (d) solution from c after a 1-electron reduction at −0.9 V, and (e) Solution from c after a 2-electron reduction at −0.9 V. Starting potential: 0.2 V.

UV−vis (characteristic band at 460 nm) and ^{31}P NMR (δ = −9.8 ppm) spectroscopy confirm the presence of $[Pd_3(Cl)]^+$. Suspecting the presence of the highly reactive zerovalent species such as $Pd_2(dppm)_2$ or Pd(dppm) (these species may be in equilibrium, as mentioned for the related ligands dcpe and dppe),[14] we evaporated the crude product under Ar and recorded the ^{31}P NMR spectrum using $CDCl_3$ to induce an oxidative addition that produces $Pd(dppm)Cl_2$. The reaction of dihalomethanes with a binuclear palladium(0) complex was reported.[15] The other signal, in addition ot the resonance at −9.8 ppm discussed above, is indeed at −56.3 ppm (singlet) as verified with an authentic sample.[11] The zerovalent species $Pd_2(dppm)_3$[16] formed according to reaction 8 was detected by ^{31}P NMR (δ = 12.4 ppm) and electrochemistry (oxidation wave at −0.23 V) after the addition of an excess of dppm in solution.[7]

$$2[Pd_3]^+ + Pd_2(dppm)_2Cl_2 + dppm \rightarrow 2[Pd_3Cl]^+ + Pd_2(dppm)_3 \quad (8)$$

The overall result can be interpreted by electron−ligand exchange reaction 9

$$2[Pd_3]^+ + Pd_2(dppm)_2Cl_2 \rightarrow 2[Pd_3Cl]^+ + Pd_2(dppm)_2 \quad (9)$$

The outer-sphere electron transfer between Pd_2Cl_2 and $[Pd_3]^+$ is impossible on the basis of the redox potentials (the difference of 0.84 V is too large). However, the cationic dimer $[Pd_2Cl]^+$ should be more easily reduced than Pd_2Cl_2[13] and can be reduced by $[Pd_3]^+$. A possible mechanism can be formulated to reactions 10 and 11 or 12. Equation 10 corresponds to a redox reaction, and 11 corresponds to the

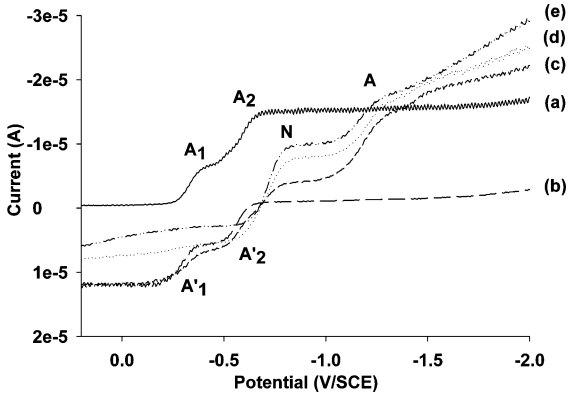

Figure 6. (a) RDE voltammograms of $[Pd_3]^{2+}$ (scan rate = 0.02 V s^{-1}) in THF/Bu_4NPF_6 solution at room temperature, (b) after a 2-electron reduction at −1 V and (c) that shown in trace b after the addition of 1 equiv of Pd_2Cl_2, (d) that shown in trace c after evolution for 30 min, and (e) that shown in trace c after 2.5 h. Starting potential: 0.2 V.

reactivity between two paramagnetic species (probably very fast)

$$Pd_2(dppm)_2Cl(THF)^+ + 2[Pd_3]^+ + Cl^- \rightarrow Pd_2(dppm)_2(Cl)THF + [Pd_3Cl]^+ \quad (10)$$

$$Pd_2(dppm)_2Cl(THF) + 2[Pd_3]^+ \rightarrow Pd_2(dppm)_2 + [Pd_3Cl]^+ + THF \quad (11)$$

$$Pd_2(dppm)_2Cl(THF)^+ + 2[Pd_3]^+ + Cl^- \rightarrow Pd_2(dppm)_2 + THF + 2\,[Pd_3Cl]^+ \quad (12)$$

The driving force of the reaction is the great stability of adduct $[Pd_3(Cl)]^+$.[2d] Stabilization of paramagnetic M−M bonded dimers, notably for d^6−d^7 Pt_2 systems, was observed before.[17]

Reactivity of $[Pd_3]^0$ toward Pd_2Cl_2. Figure 6 exhibits the RDE voltammogram of $[Pd_3]^0$ (generated from the 2-electron reduction of $[Pd_3]^{2+}$). Two oxidation waves A'_1 and A'_2 are present (trace b). After the addition of 1 equiv of Pd_2Cl_2, waves A'_1 and A'_2 disappear slowly over a period of 30 min (trace c). At this point, the reduction waves N and A and the oxidation wave N′ are observed (trace d). Again, the UV−vis and ^{31}P NMR spectra confirm the presence of $[Pd_3(Cl)]^+$, and NMR evidence confirms that of $Pd(dppm)Cl_2$, after treatment of the crude product with $CDCl_3$ (peak at −56.0 ppm). In the presence of dppm, the reaction yields $Pd_2(dppm)_3$ (^{31}P NMR singlet at 12.4 ppm in acetone-d_6 and oxidation wave −0.23 V vs SCE confirmed with an authentic sample).[7]

In the presence of 0.5 equiv of Pd_2Cl_2, the reaction is not quantitative and waves A'_1 and A'_2 are still observed even after several hours. This process is summarized by eq 13

$$2[Pd_3]^0 + Pd_2(dppm)_2Cl_2 \rightarrow [Pd_3Cl]^+ + Pd_2(dppm)_2 + Cl^- \quad (13)$$

(14) (a) Reid, S. M.; Fink, M. J. *Organometallics* **2001**, *20*, 2959. (b) Landtiser, R.; Pan, Y.; Fink, M. J. *Phosphorus, Sulfur Silicon Relat. Elem.* **1994**, *93*−*94*, 393.

(15) For examples, see: (a) Tsubomura, T.; Itsuki, A.; Homma, M.; Sakai, K. *Chem. Lett.* **1994**, 661. (b) Balch, A. L.; Hunt, C. T.; Lee, C.-L.; Olmstead, M. M.; Farr, J. P. *J. Am. Chem. Soc*. **1981**, *103*, 3764.

(16) Lindsey, C. H.; Benner, L. S.; Balch, A. L. *Inorg. Chem.* **1980**, *19*, 3503.

(17) Bennett, M. A.; Bhargava, S. K.; Boas, J. F.; Boeré, R. T.; Bond, A. M.; Edwards, A. J.; Guo, S.-X.; Hammerl, A.; Pilbrow, J. R.; Priver, S. H.; Schwerdtfeger, P. *Inorg. Chem.* **2005**, *44*, 2472.

Scheme 1

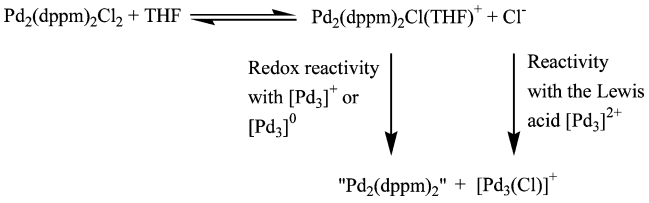

Scheme 2

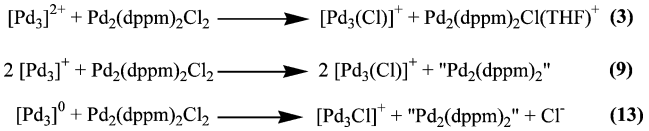

We suggest that the key step is an electron-ligand exchange reaction[4] taking place between the intermediate compound $[Pd_2Cl]^+$ and the zerovalent cluster $[Pd_3]^0$

$$[Pd_3]^0 + [Pd_2(dppm)_2(THF)Cl]^+ \rightarrow [Pd_3Cl]^+ + Pd_2(dppm)_2 + THF \quad (14)$$

Again, the stability of $[Pd_3(Cl)]^+$ must drive (as the binding constant is very large)[2d] the reaction, and in this case, $[Pd_3]^{2+}$ mediates the reduction of Pd_2Cl_2.

As mentioned, coulometry reproducibly indicates a transfer of more than 2 electrons for the $[Pd_3]^{2+}$ and Pd_2Cl_2 (between 2.6 and 3.0) using the reduction potential at wave N. This can now be explained by the subsequent reactivity of $[Pd_3]^0$ with Pd_2Cl_2.

Clearly, the stronger Lewis acidity of $[Pd_3]^{2+}$ toward Cl^- drives the reaction between $[Pd_3]^{2+}$ and Pd_2Cl_2, while the reducing ability of the paramagnetic species $[Pd_3]^+$ and zerovalent cluster $[Pd_3]^0$ toward $[Pd_2Cl]^+$ is involved when these reduced species are electrogenerated in situ. Scheme 1 summarizes the results.

The reactions describing the overall reactivities of $[Pd_3]^{2+}$, $[Pd_3]^+$, and $[Pd_3]^0$ toward Pd_2Cl_2 are summarized in Scheme 2.

Conclusion

This halide-abstraction reactivity from an inorganic molecule by the strong Lewis acid $[Pd_3]^{2+}$ (which is known for C−X bond cleavage) is new. Indeed, in the absence of direct interactions of the Pd−Cl fragment of Pd_2Cl_2 with the Pd_3^{2+} center inside the cavity because of steric interactions indicates that the mechanism proceeds via a dissociative mechanism where the uncoordinated Cl^- ion is competitively abstracted by Pd_3^{2+} rather than $Pd_2(dppm)_2Cl^+$ (back reaction). This reactivity also operates for its corresponding reduced forms ($[Pd_3]^+$ and $[Pd_3]^0$) for which the strong stability of $[Pd_3Cl]^+$ drives the reactions. Notably, in the case of the non-redox-active Ag^+ cation, only the Pd_2Cl^+ species is obtained. In addition, this latter reaction is stoichiometric only. These new results suggest that halide abstraction from Pd_2Cl_2 can be mediated by $[Pd_3Cl]^+$ which is electrochemically reduced to $[Pd_3]^0$ at a much lower potential than that of Pd_2Cl_2 (Scheme 3). Useful electrochemically assisted catalytic processes are clearly in sight in this area using $[Pd_3]^{2+}$ and its related derivatives. In this particular example, the highly reactive zerovalent $Pd_2(dppm)_2$ can be generated in situ without using chemical[18] or photochemical processes, at relatively low reductive potentials (without reducing the organics). This process involves the 2-electron reduction of $[Pd_3Cl]^+$ to form the active species $[Pd_3]^0$ which reduces Pd_2Cl_2 as shown below.

Scheme 3

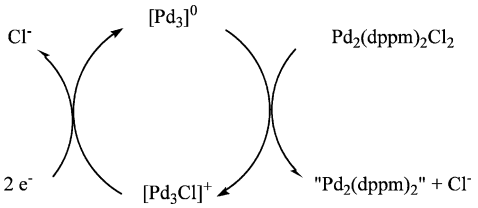

Scheme 4

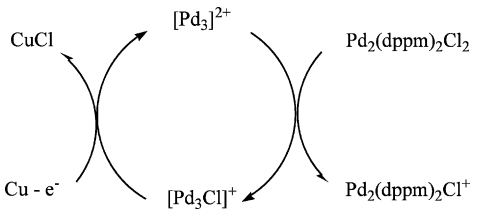

The catalytic formation of $[Pd_2Cl]^+$ can be also obtained using a sacrificial copper anode, as already mentioned in the acylchloride activation, which involved the electrochemical regeneration of the $[Pd_3]^{2+}$ dication from $[Pd_3Cl]^+$ and the precipitation of CuCl.[3b,3d]

This methodology is currently being tested using other organometallic precursors along with the testing of organic reactions mediated by the electrochemically assisted generation of the active intermediates.

Acknowledgment. P.D.H. thanks NSERC (Natural Sciences and Engineering Research Council of Canada) for funding. Y.M. is grateful to CNRS (Centre National de la Recherche Scientifique) for funding. We are grateful to Dr Jean-Michel Barbe (LIMBRES, Dijon) for MALDI-TOF experiments.

Supporting Information Available: MALDI-TOF spectrum of $[Pd_2(dppm)_2(THF)(Cl)]^+$. This material is available free of charge via the Internet at http://pubs.acs.org.

IC061777H

(18) Pan, Y.; Mague, J. T.; Fink, M. J. *J. Am. Chem. Soc.* **1993**, *115*, 3842.